

# Synthesis and Characterization of Zr(IV) Polyoxotungstates as Molecular Analogues of Zirconia-Supported Tungsten Catalysts

Richard Villanneau,<sup>\*,†</sup> Hugo Carabineiro,<sup>#</sup> Xavier Carrier,<sup>\*,‡</sup> René Thouvenot,<sup>†</sup> Patrick Herson,<sup>†</sup> Francisco Lemos,<sup>#</sup> Fernando Ramôa Ribeiro,<sup>#</sup> and Michel Che<sup>‡,¶</sup>

Laboratoire de Chimie Inorganique et Matériaux Moléculaires (UMR 7071, CNRS); Université Pierre & Marie Curie, 4 place Jussieu, 75252 Paris Cedex 05, France; Centro de Engenharia Biológica e Química, Instituto Superior Técnico, Universidade Técnica de Lisboa, Av. Rovisco Pais, 1049-001 Lisboa, Portugal; and Laboratoire de Réactivité de Surface (UMR 7609, CNRS), Université Pierre & Marie Curie, 4 place Jussieu, 75252 Paris Cedex 05, France

Received: April 5, 2004

A new zirconium-containing polyoxotungstate  $[\{W_5O_{18}Zr(\mu-OH)\}_2]^{6-}$  **2** was prepared by alkalization of a solution of the monomeric form  $[W_5O_{18}Zr(H_2O)]^{2-}$  **1**. The crystal structure of  $(nBu_4N)_6[\{W_5O_{18}Zr(\mu-OH)\}_2] \cdot 2H_2O$  (monoclinic; space group  $C2/c$ ;  $a = 26.086$ ,  $b = 17.018$ ,  $c = 32.891$  Å;  $\beta = 112.23^\circ$ ) reveals that two Lindqvist-type units  $\{ZrW_5O_{18}\}^{2-}$  (shortly  $ZrW_5$ ) are linked through two hydroxo bridges ( $Zr-OH-Zr$ ) with Zr in sevenfold coordination. Both compounds **1** and **2** were characterized by IR and Raman spectroscopy. EXAFS analysis of **1** at the W  $L_{III}$ -edge agrees with the hypothesis of a monosubstituted Lindqvist structure. The  $^{183}W$  NMR spectrum of **2** in acetonitrile is consistent with the solid-state structure assuming a dynamic process implying likely the  $\mu$ -hydroxo bridge. A brief discussion is given on the relevance of molecular zirconium-containing polyoxotungstates to heterogeneous catalysis since these compounds can be envisioned as molecular analogues of zirconia-supported tungsten catalysts.

## Introduction

High-octane gasolines are obtained through skeletal isomerization of light  $n$ -alkanes with acid catalysts, including primarily liquid acids such as  $AlCl_3/HCl$  or solid acids such as chlorinated alumina that will have to be replaced for environmental reasons.<sup>1</sup> Hence, the design of halide-free solid acid catalysts is a major industrial and environmental challenge for the petroleum refining industry. Zirconia-supported tungsten-based catalysts ( $WO_x/ZrO_2$ ) were proposed as interesting candidates by Hino and Arata<sup>2,3</sup> in the late 80's. However, despite numerous studies on  $WO_x/ZrO_2$  catalysts and convincing attempts to describe the tungsten surface phase,<sup>4–8</sup> the generation and location of acid sites on these types of catalysts are still open to discussion. No conclusive answer has been found as yet. It has even been proposed recently that the catalytic activity of tungstated zirconia is not only dependent on the acidic nature of the catalysts but also on the redox properties of tungsten.<sup>5,9</sup>

The use of molecular models for poorly defined zirconia-supported tungsten catalysts could open a new research route for gaining a fundamental understanding of this important class of solid acid catalysts. In this respect, polyoxometalates (POMs) are frequently regarded as molecular fragments of extended metal oxide structures<sup>10–13</sup> and hence, Zr-containing polyoxotungstates could serve as soluble analogues of heterogeneous tungstated zirconia catalysts. Surprisingly, Zr-containing isopolyanions have been seldom reported in the literature to date.<sup>14–16</sup>

However, in what was probably the first paper to deal with zirconotungstic polyoxoanions<sup>17</sup> the author prepared this compound (claimed to be a zirconodecatungstate) by boiling ammonium paratungstate with gelatinous zirconia, which closely resembles the preparation of  $WO_x/ZrO_2$  catalysts.<sup>6</sup> Pope<sup>15</sup> mentioned the potential formation of a decatungstate made up of a central Zr in eightfold coordination connecting two  $[W_5O_{18}]^{6-}$  groups (lacunary derivatives of the Lindqvist structure  $[W_6O_{19}]^{2-}$ ) by comparison with lanthanide (Ln) containing polyoxotungstate ( $[LnW_{10}O_{36}]^{8-}$ ).<sup>18,19</sup> However, the structural analogy between lanthanotungstates and zirconotungstates, based on results obtained by Marcu et al.<sup>20</sup> and Ripan et al.,<sup>21</sup> has never been confirmed.

Another type of Zr-containing polyoxotungstate has been reported by Chauveau et al.<sup>22</sup> with a tentative formula:  $[ZrW_5O_{19}H_2]^{2-}$  (hereafter referred to as  $ZrW_5$ ). It was proposed that this compound adopts the Lindqvist-type structure of the hexatungstate  $[W_6O_{19}]^{2-}$  anion with a  $\{Zr(H_2O)\}^{4+}$  group formally replacing one  $\{WO\}^{4+}$  group. However, the crystal structure of this compound has never been solved and the  $^{183}W$  NMR data presented by the authors had some weaknesses (low signal-to-noise ratio and incorrect intensity ratio), casting doubt on the structure of  $ZrW_5$ . Chauveau et al.<sup>22</sup> did not succeed in obtaining other polytungstates that would contain higher amounts of Zr.

More recently, Errington et al.<sup>23</sup> attempted to prepare the alkoxide-derivative of  $ZrW_5$ ,  $[(MeO)ZrW_5O_{18}]^{3-}$ , via a non-aqueous preparation method (hydrolysis of  $WO(OMe)_4$  in the presence of  $[Zr(OPr^i)_4(Pr^iOH)]$  in acetonitrile) in a controlled atmosphere using Schlenk techniques. However, this methodology did not allow them to obtain this compound;<sup>24</sup> instead, Errington has recently claimed the existence of a methoxide dimeric polyoxotungstate:  $[\{ZrW_5O_{18}(\mu-OMe)\}_2]^{6-}$ .<sup>16</sup>

This paper describes the first successful aqueous preparation and X-ray crystal structure determination of a dimeric Zr-

<sup>†</sup> Laboratoire de Chimie Inorganique et Matériaux Moléculaires, Université Pierre & Marie Curie.

<sup>#</sup> Instituto Superior Técnico, Universidade Técnica de Lisboa.

<sup>‡</sup> Laboratoire de Réactivité de Surface, Université Pierre & Marie Curie.

<sup>¶</sup> Institut Universitaire de France.

\* To whom correspondence may be addressed: Phone: 33 1 44 27 60 05. Fax: 33 1 44 27 60 33. E-mail addresses: carrier@ccr.jussieu.fr, villanne@ccr.jussieu.fr.

containing polyoxotungstate,  $[\{W_5O_{18}Zr(\mu-OH)\}_2]^{6-}$ , from condensation of Chauveau's  $[W_5O_{18}Zr(H_2O)]^{2-}$  monomers. A brief discussion is given on the potential analogy between molecular Zr-containing polyoxotungstates and zirconia-supported tungsten catalysts.

## Experimental

**Preparation of the Compounds.** Reagent grade solvents (acetonitrile and dimethyl ether) and compounds ( $ZrOCl_2 \cdot 8H_2O$ ,  $Na_2WO_4 \cdot 2H_2O$ , tetramethylammonium chloride (TMACl), tetrabutylammonium bromide (TBABr), tetrabutylammonium hydroxide (TBAOH) and  $Na_2SO_4$ ) were purchased from Aldrich, ACROS Organics, or Fluka and used as received.

(1)  $[W_5O_{18}Zr(H_2O)]^{2-}$ . The tetramethylammonium (TMA) salt of  $[W_5O_{18}Zr(H_2O)]^{2-}$  (**1**) was obtained by self-condensation of sodium tungstate with  $ZrOCl_2 \cdot 8H_2O$  in acidic medium as described by Chauveau et al.<sup>22</sup>  $ZrOCl_2 \cdot 8H_2O$  (1.288 g, 0.004 mole) was dissolved in 500 mL of a molar solution of  $Na_2SO_4$ , the pH of which was first adjusted to 2 with sulfuric acid. The resulting solution was then diluted to 800 mL with distilled water (solution A). A second solution was prepared by dissolving 0.02 mole of  $Na_2WO_4 \cdot H_2O$  (6.60 g) in 70 mL of water. This solution was then brought to the boil and 8 mL of HCl (5 mol·L<sup>-1</sup>, e.g., 0.04 mol) were added under vigorous stirring. The solution was then cooled in an ice bath (solution B). The cold solution B was added to solution A under stirring and the mixture was allowed to stand at room temperature for 3 days; 4 g of tetramethylammonium chloride were then added, leading to the slow crystallization of **1**. TGA results show that **1** does not contain crystallization water molecules. After 2 days, 3.32 g of **1** was then collected, yielding 57% based on Zr.

**1** IR (KBr):  $\nu = 3030$  (w), 963 (s), 945 (s) (TMA cation), 930 (sh) (TMA cation), 855 (sh), 815 (br), 685 (m), 665 (sh), 640 (s), 555 (m), 465 (m), 420 (s), 345 (w) cm<sup>-1</sup>,  $C_8H_{26}N_2O_{19}W_5Zr_1$ : calcd C 6.56, H 1.79, N 1.91, W 62.76, Zr 6.23; found C 5.84, H 2.12, N 1.66, W 57.87, Zr 5.78. Crystallographic data: orthorhombic, space group: *Cmm2*,  $a = 10.827(5)$ ,  $b = 15.052(6)$ ,  $c = 15.662(9)$  Å,  $V = 2552(2)$  Å<sup>3</sup>.

(2)  $[\{W_5O_{18}Zr(\mu-OH)\}_2]^{6-}$ . The TBA salt of this anion (compound **2**) is obtained by adding an aqueous solution of TBAOH to a suspension of **1** in water; 1.53 mL of a 1.5 mol·L<sup>-1</sup> solution of TBAOH in water (2.30 mmol) was added to a suspension of 1.68 g (1.13 mmol) of **1** in 50 mL of distilled water (pH = 4). The suspension was stirred at room temperature until dissolution of the solid. After separation of a very fine undissolved powder, the resulting solution was allowed to slowly evaporate at 70 °C. During this period, large and colorless crystals of **2**·2H<sub>2</sub>O suitable for X-ray diffraction analysis formed. They were collected and dried with dimethyl ether. Next, 1 g of tetrabutylammonium bromide was added to the liquor-solution, resulting in further precipitation of **2** (total yield: 0.89 g, 39%) after stirring for 1 day.

IR (KBr):  $\nu = 3680$  (m), 970 (w), 945 (s), 880 (m), 810 (br), 730 (s), 640 (m), 555 (m), 435 (s), 420 (sh) cm<sup>-1</sup>; <sup>183</sup>W NMR (12.5 MHz, CD<sub>3</sub>CN, 300 K)  $\delta = 73.6$  (s, <sup>2</sup> $J_{W-W} = 6.2$  Hz), 47.9 (s, <sup>2</sup> $J_{W-W} = 6.2$  Hz),  $C_{96}H_{222}N_6O_{40}W_{10}Zr_2$ : calcd C 27.97, H 5.43, N 2.04, W 44.60, Zr 4.43; found C 27.93, H 5.40, N 2.04, W 42.56, Zr 4.18.

**IR Spectroscopy.** IR spectra were recorded from KBr pellets on a Bio-rad Win-IR FTS 165 FT-IR spectrophotometer.

**Raman Spectroscopy.** Raman spectra were collected with a Kaiser Optical Systems HL5R Raman spectrometer equipped with a near-IR laser diode working at 785 nm. The laser power

was adjusted to 10–15 mW at the sample position for all spectra. The average resolution is equal to 3 cm<sup>-1</sup>.

**<sup>183</sup>W NMR spectra.** <sup>183</sup>W spectra were recorded in 10-mm o.d. tubes at 12.5 MHz on a Bruker AC 300 spectrometer equipped with a low-frequency special VSP probehead. Chemical shifts are given with respect to an external 2 M Na<sub>2</sub>WO<sub>4</sub> solution in alkaline D<sub>2</sub>O, using a saturated aqueous solution of dodecatungstosilicic acid (SiW<sub>12</sub>O<sub>40</sub>H<sub>4</sub>) as a secondary standard ( $\delta = -103.8$  ppm).

**Analyses.** Elemental analyses were performed by the Service de Microanalyses (Université Pierre et Marie Curie, Paris, France) and the Laboratoire Central d'Analyses du CNRS (Vernaison, France).

**X-ray Absorption Spectroscopy.** XAS data were collected at the Laboratoire pour l'Utilisation du Rayonnement Electromagnétique (LURE, France) on beamline D42 using channel-cut silicon (111) crystals. The electron energy and ring current were 1.85 GeV and 250 mA, respectively. The W L<sub>III</sub>-edge spectrum of compound **1** was recorded in the transmission mode in air at 77 K with ion chambers. The sample was thoroughly ground and mixed with cellulose and pressed in the form of a pellet to get an absorption coefficient  $\mu$  of 2–3 at the W L<sub>III</sub>-edge. Calibration of the monochromator was performed with a W-metal foil. The energy was scanned with incremental energy steps of 2 eV/point from 10 100 to 10 200 eV, 1 eV/point from 10 200 to 10 350 eV, and 2 eV/point from 10 350 to 11 000 eV; 2 scans were collected for an analysis time of about 1 h.

EXAFS data extraction was performed by standard procedures<sup>25</sup> using Michalowicz's software package.<sup>26,27</sup> Fourier Transforms (FT) of  $w(k)k^3$ .  $\chi(k)$  EXAFS data ( $w(k)$  is a Kaiser-Bessel window with a smoothness parameter of 3) were then carried out in the range 3.6–15.0 Å<sup>-1</sup> in order to obtain a radial distribution function (RDF). Each coordination shell of the RDF was then filtered using inverse Fourier transformation and  $k^1$ -weighted Fourier filtered data were fitted in  $k$ -space. Fourier transformation and Fourier filtering were conducted using "EXAFS98" and multiple shell fitting was carried out with "Round Midnight".<sup>26,27</sup> The quality of the fit was estimated by the agreement factor:<sup>27</sup>

$$\rho(\%) = \frac{\sum [k\chi_{\text{exp}}(k) - k\chi_{\text{th}}(k)]^2}{\sum [k\chi_{\text{exp}}(k)]^2} \quad (1)$$

**Crystal Structure Analysis.** Data for **2**·2H<sub>2</sub>O were recorded at room temperature on a Kappa-CCD Bruker diffractometer with graphite monochromated MoK $\alpha$  radiation ( $\lambda = 0.71073$  Å) and the  $\omega$ -scan technique. Orientation matrix and lattice parameters were obtained by least-squares refinement of the diffraction data of 98 reflections within the range of  $6^\circ < \theta < 18^\circ$ . The index ranges of data collection were  $-33 \leq h \leq 32$ ,  $-19 \leq k \leq 22$ , and  $-42 \leq l \leq 42$ . Intensity data were collected in the  $\theta$  range 2.0–27.5°, 6336 reflections have  $(Fo)^2 \geq 3\sigma(Fo)^2$ . All the measured independent reflections were used in the analysis. The structure was solved by direct methods and refined with full-matrix least-squares technique on  $F$  using the SHELXS-97<sup>28</sup> and CRYSTALS<sup>29a</sup> programs. All non-hydrogen atoms were refined anisotropically, except for the tetrabutylammonium cations and the solvent molecules. Hydrogen atoms were not included in the refinements. The values of the discrepancy indices R1 ( $R_w$ ) for all data were 0.1152 (0.0928). The final Fourier-difference map showed maximum and minimum peaks height of 1.91 and  $-1.44$  e.Å<sup>-3</sup>. The number of variable parameters is 434, and the value of the goodness-of-fit is 1.079. The molecular structure was drawn with the program CAMERON.<sup>29b</sup> CCDC 229907 contains the supplementary crystallographic data for this paper. These data

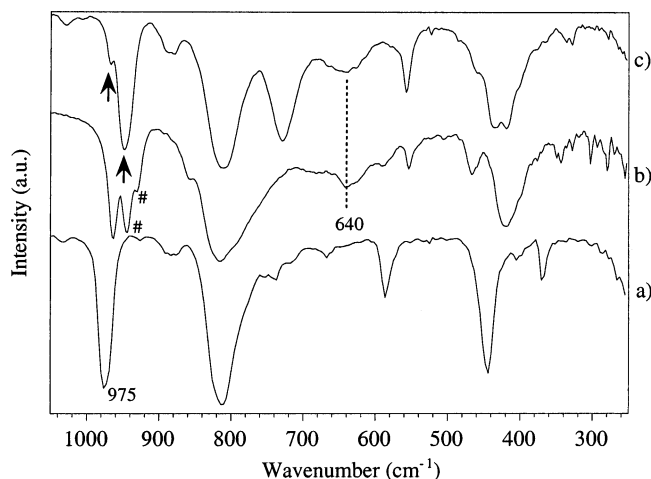
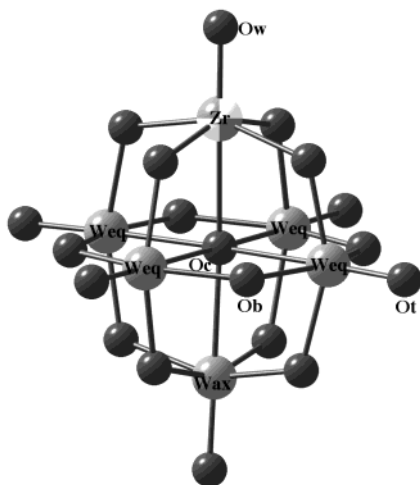


**Figure 1.** Infrared spectra (KBr technique) of (a)  $(\text{TBA})_2[\text{W}_6\text{O}_{19}]$ , (b)  $(\text{TMA})_2[\text{W}_5\text{O}_{18}\text{Zr}(\text{H}_2\text{O})]$  (**1**), and (c)  $(\text{TBA})_6\{[\text{W}_5\text{O}_{18}\text{Zr}(\mu\text{-OH})]_2\}$  (**2**). #TMA cation. The arrows are indicative of the splitting of the  $\nu\text{W}=\text{O}_t$  vibration mode.

### SCHEME 1: Idealized Representation of the $[\text{W}_5\text{O}_{18}\text{Zr}(\text{H}_2\text{O})]^{2-}$ Anion **1**



can be obtained free of charge via [www.ccdc.cam.ac.uk/conts/retrieving.html](http://www.ccdc.cam.ac.uk/conts/retrieving.html) (or from the Cambridge Crystallographic Data Centre, 12 Union Road, Cambridge CB2 1EZ, United Kingdom; fax: (+44)1223-336-033; e-mail: [deposit@ccdc.cam.ac.uk](mailto:deposit@ccdc.cam.ac.uk)).

## Results and Discussion

A schematic representation of the Lindqvist-type anion of **1** is given in Scheme 1. The different atoms are labeled according to their position in the structure:  $\text{O}_t$ ,  $\text{O}_b$ , and  $\text{O}_c$  are terminal, bridging, and central oxygens, respectively, while  $\text{O}_w$  stands for a water molecule.  $\text{W}_{\text{ax}}$  and  $\text{W}_{\text{eq}}$  are axial and equatorial tungsten atoms.

**Infrared and Raman Spectroscopy.** The IR spectra of compounds **1** and **2** (Figure 1b and 1c respectively) are typical of monosubstituted Lindqvist-type polyoxoanions.<sup>30–32</sup> The spectrum of the complete  $[\text{W}_6\text{O}_{19}]^{2-}$  displays a single and highly symmetric band at  $975\text{ cm}^{-1}$  ( $\nu\text{W}=\text{O}_t$ ) (Figure 1a),<sup>33</sup> while the corresponding  $\nu\text{W}=\text{O}_t$  mode for compound **2** gives rise to a double band (see the arrows in Figure 1c). This splitting is in agreement with a loss of the  $\text{O}_h$  symmetry for the Lindqvist structure due to the incorporation of  $\text{Zr}^{\text{IV}}$  in place of a  $\text{W}^{\text{VI}}$  cation in the parent compound  $[\text{W}_6\text{O}_{19}]^{2-}$ . The splitting of this band is not observed in the case of **1** but a detailed analysis of the

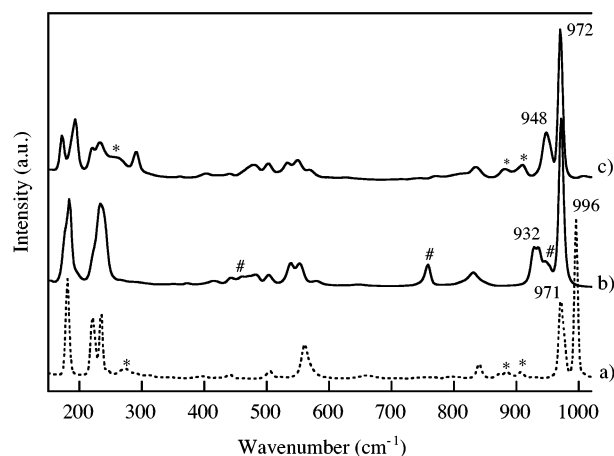


**Figure 2.** Solid-state Raman spectra of (a)  $(\text{TBA})_2[\text{W}_6\text{O}_{19}]$ , (b)  $(\text{TMA})_2[\text{W}_5\text{O}_{18}\text{Zr}(\text{H}_2\text{O})]$  (**1**), and (c)  $(\text{TBA})_6\{[\text{W}_5\text{O}_{18}\text{Zr}(\mu\text{-OH})]_2\}$  (**2**). \*TBA and #TMA cation.

$1000\text{--}900\text{ cm}^{-1}$  region is not possible due to the presence of several bands assigned to the TMA counteranion. The  $\nu\text{W}=\text{O}_t$  wavenumber for  $[\text{W}_6\text{O}_{19}]^{2-}$  is higher than that of **1** and **2**, which is in agreement with previous results obtained on  $\text{Nb}^{\text{V}}$  or  $\text{Mo}^{\text{V}}$  derivatives.<sup>30–32</sup> The introduction of a cation with a smaller oxidation state and a higher ionic radius ( $72\text{ pm}$  for  $\text{Zr}^{\text{IV}}$  and  $60\text{ pm}$  for  $\text{W}^{\text{VI}}$ ) decreases the cohesion of the framework, which induces a decrease of the force constant for the  $\text{W}=\text{O}_t$  bonds.

The band that is observed at  $640\text{ cm}^{-1}$  for **1** was assigned to a  $\text{Zr}-\text{O}_b$  vibration (i.e.,  $\nu_{\text{Zr}-\text{O}-\text{W}}$ ) by Chauveau et al.<sup>22</sup> since this band is absent for  $[\text{W}_6\text{O}_{19}]^{2-}$ . However, this assignment may be ruled out since a band at  $640\text{ cm}^{-1}$  is also observed for **2** while a  $\text{Zr}-\text{O}_b$  vibration should be strongly modified in the monomer (**1**) and in the dimer (**2**).

The IR spectra of **1** and **2** present high frequency  $\nu_{\text{OH}}$  bands (not shown) at  $3030$  and  $3680\text{ cm}^{-1}$ , respectively, indicating the presence of either aqua (**1**) or hydroxo (**2**) ligands bound to the  $\text{Zr}^{\text{IV}}$  cation.

The same general trends are observed for the Raman spectra obtained for compounds **1** and **2** (Figure 2). The Raman spectrum of the hexatungstate, also reported for comparison, shows two bands at  $996$  and  $971\text{ cm}^{-1}$  that are assigned to symmetric and antisymmetric  $\text{W}=\text{O}_t$  stretchings, respectively.<sup>31,33</sup> The  $\nu_s(\text{W}=\text{O}_t)$  mode shifts to lower wavenumbers ( $972\text{ cm}^{-1}$ ) when a  $\text{W}^{\text{VI}}$  atom is replaced by  $\text{Zr}^{\text{IV}}$  in the Lindqvist structure in agreement with IR data and previous Raman studies on Nb-substituted hexatungstates.<sup>30</sup> The  $\nu_{\text{as}}(\text{W}=\text{O}_t)$  mode appears as a poorly resolved doublet centered at  $932\text{ cm}^{-1}$  for **1**. The splitting of this mode may be explained by the loss of the  $\text{O}_h$  symmetry. Conversely, the same mode appears as a single band at higher wavenumber ( $948\text{ cm}^{-1}$ ) for **2**.

As regards  $\text{Zr}-\text{O}$  vibrations, they are expected to be located below  $640\text{ cm}^{-1}$  by reference to zirconium dioxide.<sup>34</sup> However, it is not straightforward to assign any of the Raman bands to a specific  $\nu_{\text{Zr}-\text{O}}$  vibration since none of the bands for **1** and **2** are clearly distinct from those observed for the hexatungstate. A slight difference between  $[\text{W}_6\text{O}_{19}]^{2-}$  and Zr-containing compounds arises from the complex pattern observed between  $450$  and  $550\text{ cm}^{-1}$ . However, this broad pattern was previously observed for Nb-substituted hexatungstates<sup>30</sup> and thus, it seems doubtful to conclude on the assignment of bands to  $\text{Zr}-\text{O}$  vibrations without additional experiments.

**$^{183}\text{W}$  NMR.** The very low solubility of **1** prevented the obtaining of its  $^{183}\text{W}$  NMR spectrum. On the contrary, **2** is sufficiently soluble in acetonitrile to get a  $^{183}\text{W}$  spectrum with



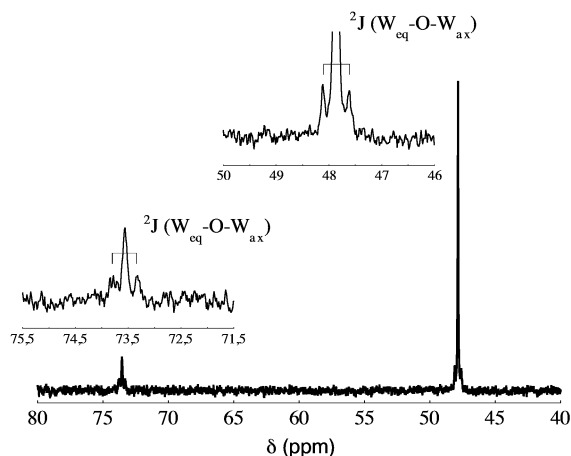


**Figure 3.** 12.5 MHz  $^{183}\text{W}$  NMR spectrum of an 0.133 mol.L $^{-1}$   $\text{CH}_3\text{CN}/\text{CD}_3\text{CN}$  solution of  $(\text{TBA})_6[\{\text{W}_5\text{O}_{18}\text{Zr}(\mu\text{-OH})_2\}]$  (**2**) at 300 K, with abscissa expansion of each line showing the tungsten satellites. Using 20  $\mu\text{s}$  pulses (ca 45° flip angle) with a spectral width of 750 Hz (60 ppm), 1500 transients were recorded. For 8 K data points, the acquisition time of 5.46 s did not require additional relaxation delay and the digital resolution after Fourier transformation amounts 0.18 Hz/Pt. Total spectrometer time: 2 h 15 min.

good signal-to-noise ratio in moderate spectrometer time (see the caption of Figure 3). The spectrum of **2** consists of two resonances at +73.6 and +47.9 ppm, in the intensity ratio 1:4, that can be assigned to axial ( $\text{W}_{\text{ax}}$ ) and equatorial ( $\text{W}_{\text{eq}}$ ) W atoms in monosubstituted hexatungstate. This spectrum is reminiscent of that published by Chauveau et al.<sup>22</sup> (+45 and +34.6 ppm) for the postulated monomeric  $(\text{TBA})_2[\text{ZrW}_5\text{O}_{18}(\text{H}_2\text{O})]$  ( $\text{TBA-ZrW}_5$ ). However, in addition to the chemical shift differences, these spectra also differ by the spectral resolution. The  $^{183}\text{W}$  NMR spectrum of  $\text{TBAZrW}_5$  reported by Chauveau et al.<sup>22</sup> presents two broad signals with the less intense one hardly discernible from the baseline despite favorable conditions ( $10^4$  transients, high concentration 0.5 mol.L $^{-1}$  and high magnetic field 11.8 T). Conversely, the  $^{183}\text{W}$  NMR spectrum of the dimeric species (**2**) exhibits two narrow signals ( $\Delta\nu_{1/2} < 1$  Hz) with a signal-to-noise ratio that is sufficiently good to observe satellites around each principal resonance despite a lower magnetic field (7.1 T) and fewer transients (1500). These satellites are due to homonuclear coupling constants between nonequivalent  $^{183}\text{W}$  nuclei. The coupling constant value ( $^2J_{\text{W-W}} = 6.2$  Hz) is in the usual range for “edge” connections between  $\text{WO}_6$  octahedra in hetero- and isopolytungstates.<sup>35–37</sup> This value is in agreement with the  $\text{W}_{\text{eq}}\text{-O-W}_{\text{ax}}$   $\mu$ -oxo angle determined by X-ray diffraction (mean value 117.5°, see below).

It has to be noted that there is no incidence of the  $^{91}\text{Zr}$  nucleus (NA 11.23%) on the  $^{183}\text{W}$  resonances. Because of the large quadrupolar moment of  $^{91}\text{Zr}$ , the relaxation of this nucleus is expected to be very rapid, resulting in self-decoupling of the nearby  $^{183}\text{W}$  nuclei.

According to the X-ray structure (see below) the dimeric anion is located on an inversion center and the two  $\text{ZrW}_5$  units are equivalent. However, the fourfold axis ( $\text{W}_{\text{ax}}\text{-Zr}$ ) of the monosubstituted monomeric Lindqvist anions (Scheme 1) is absent in the structure of the dimeric form. In solution, the  $\text{W}_{\text{ax}}\text{-Zr-Zr-W}_{\text{ax}}$  axis may be at most a  $C_2$  axis and the overall symmetry of the anion could be  $C_{2h}$ , with a plane of symmetry perpendicular to the plane defined by the two  $\text{Zr}(\text{OH})\text{-Zr}$  bridges. Therefore the four equatorial W atoms are no longer equivalent. Depending on the relative orientation of this plane with respect to the  $\text{ZrW}_5$  framework, the equatorial W atoms may be subdivided in two (2 + 2) or three (2 + 1 + 1) types.

Accordingly, the  $^{183}\text{W}$  spectrum of the dimeric form **2** should present three or four resonances. If we reject an improbable accidental degeneracy, two different hypotheses may account for the experimental two-line spectrum: (i) different structures in solution and in the solid state or (ii), the existence of a dynamic process leading to an exchange of the equatorial tungsten atoms.

The first hypothesis may be ruled out since the Raman spectra of the solid dimer and of its acetonitrile solution are very similar. Moreover, restoring a fourfold axis in the dimeric structure implies breaking one of the  $\mu$ -hydroxo bridges, which would require addition of one  $\text{H}^+$  equivalent.

Thus, a dynamic process is likely responsible for the abnormally simple  $^{183}\text{W}$  spectrum of  $[\{\text{W}_5\text{O}_{18}\text{Zr}(\mu\text{-OH})_2\}]^{6-}$ . Observation of such spectra for monosubstituted Lindqvist anions is not unprecedented; for example, for the aryl diazenido derivatives of the hexamolybdate  $[\text{Mo}_6\text{O}_{18}(\text{N}_2\text{Ar})]^{3-}$  where fast rotation of the aryldiazenido ligand occurs in solution.<sup>38</sup> In the present case, the dynamic process likely concerns a concerted pseudorotation of the  $\mu$ -hydroxo bridges around the  $\text{Zr-Zr}$  axis. Further experiments are needed to delineate this process. Let us notice that a similar spectrum was obtained by Clegg et al.<sup>23</sup> for a compound that has been recently claimed to be a methoxide dimeric polyoxotungstate  $[\{\text{W}_5\text{O}_{18}\text{Zr}(\mu\text{-OCH}_3)_2\}]^{6-}$  anion.<sup>16</sup> In that case the dynamic process would imply  $\mu$ -methoxo bridges.

**EXAFS Spectroscopy.** Preliminary results of a single-crystal analysis of **1** (see unit cell parameters in the Experimental Section) confirmed the presence of discrete polyoxometalates. Despite repeated attempts, it has not been possible so far to obtain single crystals of **1** suitable for complete X-ray structure determination. However, to get structural information, the EXAFS spectrum (W  $L_{III}$ -edge) of **1** was recorded at 77 K. The experimental and calculated EXAFS signals and the corresponding Fourier transforms are presented in Figure 4. The results of the fit are given in Table 1. First, it was checked on the complete Lindqvist structure  $[\text{W}_6\text{O}_{19}]^{2-}$  that the contribution of the multiple scattering was negligible for this structure. Then, the coordination numbers ( $N$ ) used for the fit were fixed to the theoretical value for a monosubstituted Lindqvist structure: 1 terminal and 4 bridging oxygen atoms and 3.2 tungsten neighbors (1 axial and 4 equatorial W atoms). Only five oxygen atoms were included in the fit. Indeed, it had been previously shown by Evans et al.<sup>39</sup> that the Debye-Waller factor of the sixth W–O distance (corresponding to the central oxygen,  $\text{O}_c$ , of the Lindqvist structure) was very high, resulting in a negligible contribution of this fairly long distance (2.3 Å) to the overall fit. Taking into account these constraints, the first oxygen shell can be satisfactorily fitted with 1 terminal and 4 bridging oxygen atoms at 1.75 and 1.91 Å, respectively. Accordingly, the W–W distance is adequately fitted with 3.2 W neighbors at 3.30 Å. The introduction of a supplementary zirconium atom in the fit did not show any influence on the calculated EXAFS signal and its Fourier transform. The fitted data are in agreement with the mean crystallographic distances<sup>40</sup> for  $[\text{W}_6\text{O}_{19}]^{2-}$  and for the dimeric anion **2** (see below and Table 3). In conclusion, EXAFS data of compound **1** are in accordance with the monosubstituted Lindqvist-type structure ( $\text{ZrW}_5$ ) postulated by Chauveau et al.<sup>22</sup> An idealized representation of this compound is given in Scheme 1.

**Crystal Structure of  $2\cdot 2\text{H}_2\text{O}$ .** The asymmetric unit of  $2\cdot 2\text{H}_2\text{O}$  (Figure 5) contains one-half- $[\{\text{ZrW}_5\text{O}_{18}(\text{OH})\}]^{6-}$  anion, one molecule of solvent (water) and three tetrabutylammonium cations, all in general positions. The complete anion is located at an inversion center. According to the charge

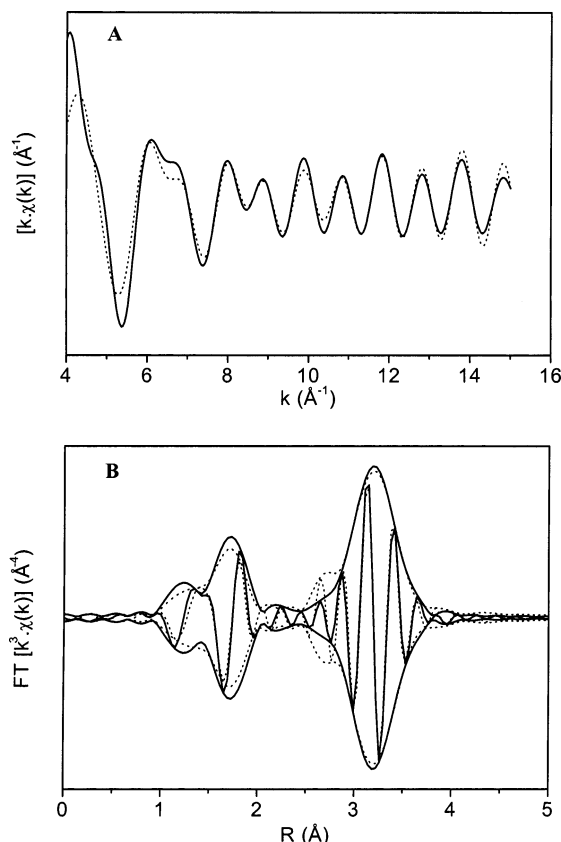


**Figure 4.** Fourier-filtered ( $R = 1.0\text{--}4.0$  Å) W  $L_{III}$  edge EXAFS spectra ( $k^3$  weighted) recorded at 77 K of  $(TMA)_2[W_5O_{18}Zr(H_2O)]$ . (A) EXAFS signal and (B) FT magnitude and imaginary part of the EXAFS function. Solid line: Fourier-filtered experimental data, dotted lines: fitted data.

**TABLE 1: EXAFS Fitting Results<sup>a</sup>**

shell	N <sup>b</sup>	R (Å)	$\sigma^2$ (Å <sup>2</sup> )	$\Delta E_0$ (eV)	$\rho$ (%)
W–O <sub>t</sub>	1	1.75	0.006	11	14.9
W–O <sub>b</sub>	4	1.91	0.0571	11	
W–W	3.2	3.30	0.0300	14	

<sup>a</sup> Standard errors in EXAFS are  $\pm 0.02$  Å in distance and  $\pm 10\%$  in coordination number. <sup>b</sup> Coordination numbers ( $N$ ) were kept fixed during the fit.

balance, one proton is associated with the  $\{ZrW_5O_{18}(OH)\}$  subunit. It was located by using Bond Valence Sum (BVS) calculations, where  $BVS = \sum BV_i = \sum \exp[(r_0 - r_i)/B]$ ,  $r_0 = 1.917$  Å for  $W^{VI}\text{--}O^{II}$ ,  $r_0 = 1.928$  Å for  $Zr^{IV}\text{--}O^{II}$ , and the empirical parameter  $B = 0.37$ .<sup>41,42</sup> The BVS values fall in the range 1.613–1.955, except for the bridging O(11), which has a BVS value equal to 1.082 and is therefore presumed to be protonated. The anion of **2** may then be viewed as the association of two  $\{ZrW_5\}$  Lindqvist-type clusters linked through two  $Zr(1)\text{--}(\mu\text{--}O(11)H)\text{--}Zr(1)'$  bridges. These  $\{ZrW_5\}$  clusters show approximately the same structural pattern as that of the complete  $[W_6O_{19}]^{2-}$ , with the notable exception of the dissymmetry of the W–O–Zr bridges, that is, significant short W–O distances (in the range 1.82–1.83 Å) with respect to the other W–O<sub>b</sub> bonds (1.90 to 1.98 Å) and large Zr–O distances (in the range 2.06–2.11 Å). In the anion of **2**, the zirconium atoms are seven-coordinated, which is common for  $Zr^{IV}$ , as shown for example in the monoclinic (baddeleyite) form of  $ZrO_2$ .<sup>43</sup> There are many examples of discrete seven-coordinated hydroxo-bridged Zr complexes in the literature. This geometry appears very usual for ZrCp-containing species but examples of nonorganometallic complexes are scarcer.<sup>16,44–49</sup>

**TABLE 2: Crystal Data for Compound  $2 \cdot 2H_2O$**

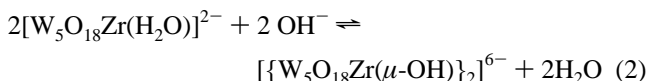
$2 \cdot 2H_2O$	
formula	$C_{96}H_{222}N_6O_{40}W_{10}Zr_2$
$Mr$ [g mol <sup>−1</sup> ]	4119.76
color	colorless
crystal system	monoclinic
space group	$C2/c$
$T$ (K)	ambient
$a$ [Å]	26.086(6)
$b$ [Å]	17.018(3)
$c$ [Å]	32.891(12)
$\alpha$ [°]	90
$\beta$ [°]	112.23(2)
$\gamma$ [°]	90
$V$ [Å <sup>3</sup> ]	13515(3)
$Z$	4
$\mu$ [cm <sup>−1</sup> ]	86.89
$\rho_{\text{calc}}$ [g cm <sup>−3</sup> ]	2.025
$\theta_{\text{min}}\text{--}\theta_{\text{max}}$ [°]	2–27.5
octants collected	−33, 32; −19, 22; −42, 42
reflections measured	46 344
unique reflections ( $R_{\text{int}}$ )	15 024 (0.066)
observed reflections	6336 ( $F_o$ ) <sup>2</sup> > $3\sigma(F_o)$ <sup>2</sup>
absorption correction	Difabs [ $T_{\text{min}}$ 0.88, $T_{\text{max}}$ 1.06]
refined parameters	434
$R$	0.0409
$R_w$	0.0465*
goodness of fit $S$	1.079
$\Delta\rho$ (max/min) [e.Å <sup>−3</sup> ]	1.91/−1.44

\*Weighting scheme of the form  $w = w'[1 - (|F_o| - |F_c|)/6\sigma(F_o)]^2$  with  $w' = 1/\sum A_i T_i(X)$  with coefficients 0.468, 0.232, and 0.278 for a Chebyshev series for which  $X = F_c/F_c(\text{max})$ .

**TABLE 3: Selected Bond Distances (Å) for Compound  $2 \cdot 2H_2O$**

W(1)–O(1)	1.69(1)	W(1)–O(12)	1.897(9)
W(1)–O(13)	1.92(1)	W(1)–O(14)	1.918(9)
W(1)–O(15)	1.91(1)	W(1)–O(2345)	2.403(8)
W(2)–O(2)	1.692(9)	W(2)–O(12)	1.970(9)
W(2)–O(21)	1.832(9)	W(2)–O(23)	1.944(9)
W(2)–O(24)	1.93(1)	W(2)–O(2345)	2.340(9)
W(3)–O(3)	1.74(1)	W(3)–O(13)	1.972(9)
W(3)–O(23)	1.927(9)	W(3)–O(31)	1.822(9)
W(3)–O(35)	1.911(9)	W(3)–O(2345)	2.306(9)
W(4)–O(4)	1.72(1)	W(4)–O(14)	1.951(9)
W(4)–O(24)	1.928(9)	W(4)–O(41)	1.834(9)
W(4)–O(45)	1.92(1)	W(4)–O(2345)	2.341(9)
W(5)–O(5)	1.691(11)	W(5)–O(15)	1.965(9)
W(5)–O(35)	1.98(1)	W(5)–O(45)	1.94(1)
W(5)–O(51)	1.830(9)	W(5)–O(2345)	2.336(9)
Zr(1)–O(11)	2.135(9)	Zr(1)–O(11)'	2.177(8)
Zr(1)–O(21)	2.107(9)	Zr(1)–O(31)	2.09(1)
Zr(1)–O(41)	2.058(9)	Zr(1)–O(51)	2.109(9)
Zr(1)–O(2345)	2.371(8)		

**Preparation of the Compounds.** Dimerization of the Lindqvist-type anion **1** is the consequence of the partial deprotonation of the water molecule bound to  $Zr^{IV}$ . It must be noted that according to reaction 2:



the dimerization reaction formally requires only one equivalent of base per monomer. Such conditions did not allow the isolation of **2**, and two equivalents of base were thus necessary. In addition, two equivalents of TBA cations (introduced with TBAOH) per  $[W_5O_{18}Zr(H_2O)]^{2-}$  units did not allow the complete precipitation of **2** since the corresponding precipitation requires three cations per  $\{W_5O_{18}Zr(\mu\text{--}OH)\}^{3-}$  subunit. Hence, to increase the yield of the reaction, it is possible to add an excess of TBABr after collecting the first crop of **2**.

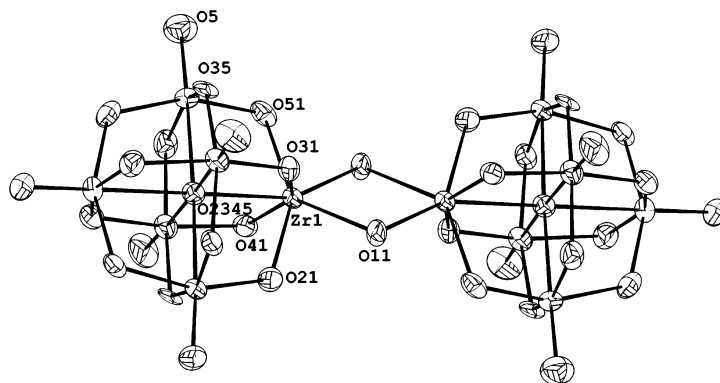


Figure 5. Molecular structure of the  $[\{W_5O_{18}Zr(\mu-OH)\}_2]^{6-}$  anion **2**.

The pH-dependent interconversion of monomers to oxo/hydroxo dimers was previously demonstrated for  $Ti^{IV}$ -containing heteropolytungstates. Kholdeeva et al.<sup>50</sup> showed that acidification of  $[PTiW_{11}O_{40}]^{5-}$  leads to the formation of a  $\mu$ -hydroxo dimer  $[(PTiW_{11}O_{39})_2OH]^{7-}$  through protonation of the  $Ti=O$  bond. Likewise, a  $\mu$ -oxo dimer of a di- $Ti^{IV}$ -substituted Keggin-type phosphotungstate  $[(P_2W_{20}Ti_4O_{78})]^{10-}$  was isolated by Nomiya et al.<sup>51</sup> in acidic solutions while the monomer was predominantly formed at near-neutral pH. These two examples show that dimerization proceeds most probably through the nucleophilic addition of an hydroxo group formed by protonation of a metal-oxo double bond in acidic conditions. In the case of Zr-containing polyoxotungstates, the reverse acido-basic behavior is observed since the monomer probably contains a water molecule bound to  $Zr^{IV}$ . Hence, the dimer is formed after deprotonation of the water molecule in alkaline conditions.

**Relevance to Heterogeneous Tungstated Zirconia Catalysts.** Following up previous work on the formation of Al-polyoxomolybdate during preparation of alumina-supported Mo catalysts,<sup>52,53</sup> Scheithauer et al.<sup>6,54</sup> suggested that the tungsten surface phase in  $WO_x/ZrO_2$  catalysts could be composed of Zr-containing polytungstates (surface pseudo-heteropolyanions). They proposed that replacement of  $W^{6+}$  by  $Zr^{4+}$  in surface polytungstates would require charge compensation by protons (as in Keggin-type heteropolyacids), providing a plausible explanation for the acidity of  $WO_x/ZrO_2$  catalysts.

This idea is also contained in the work of Barton et al.,<sup>55,56</sup> where it is suggested that the generation of Brønsted acid sites arises from a slight reduction of  $W^{6+}$  cations in the reaction mixture (containing  $H_2$  and/or hydrocarbons). The creation of this negative charge would be favored by delocalization over several  $WO_x$  neighbors (the optimum catalytic activity is thus consistent with large  $WO_x$  domains) and would require the presence of  $H^{\delta+}$  compensating species. These authors note that this creation of Brønsted acid sites is similar to the one observed for heteropolytungstic acids. Indeed,  $H_3[PW_{12}O_{40}]$  shows a strong Brønsted acidity since a small negative charge is delocalized over the twelve tungsten atoms of the  $[PW_{12}O_{40}]^{3-}$  anion, which makes this species a very weak base. Creation of Brønsted acidity through an intimate interaction between W and Zr is also contained in the proposed model of Afanasiev et al.,<sup>57</sup> since these authors describe the surface species as composed of Zr-OH groups surrounded by several W atoms containing a W-O double bond.

Hence, the availability of Zr-containing polyoxotungstates will give a fundamental basis for investigating the role of and need for an intimate interaction between zirconium and tungsten in  $WO_x/ZrO_2$  catalysts, since the compounds reported in this paper represent a new class of soluble analogues of tungstated zirconia

catalysts. They involve a variety of (i) Zr coordinations (sixfold and sevenfold for **1** and **2** respectively), (ii) cluster sizes (5 and 10 W atoms for **1** and **2**, respectively), (iii) hydroxo/aqua groups that can mimic different types of surface OH groups, and (iv) cluster charges (2- for **1** and 6- for **2**) that should influence the acidity of the acid form of the polyanions as shown earlier for Keggin-type heteropolyacids.<sup>10</sup>

## Conclusion

A straightforward aqueous preparation route is given for two zirconium-containing polyoxotungstates that have been characterized by spectroscopic methods ( $^{183}W$  NMR, IR, Raman spectroscopy, EXAFS) and X-ray crystallography. The first compound,  $[W_5O_{18}Zr(H_2O)]^{2-}$  (or  $ZrW_5$ ), adopts a Lindqvist structure that derives from the hexatungstate  $[W_6O_{19}]^{2-}$ . The second compound is a dimer,  $[\{W_5O_{18}Zr(\mu-OH)\}_2]^{6-}$ , formed from condensation of two  $ZrW_5$  monomers after controlled alkalization of the solution. The crystal structure of  $[\{W_5O_{18}Zr(\mu-OH)\}_2]^{6-}$  reveals that the two  $ZrW_5$  units are linked through two hydroxo bridges ( $Zr-OH-Zr$ ) with Zr in sevenfold coordination. To the best of our knowledge, this is the first structural characterization of this compound. Molecular Zr-containing polyoxotungstates may serve as soluble analogues of heterogeneous tungstated zirconia catalysts that are interesting environmentally friendly acid catalysts for isomerization of light *n*-alkanes.

**Acknowledgment.** The authors kindly thank J.-M. Krafft and F. Villain for their help and advice during Raman and X-ray absorption measurements, respectively. This paper is dedicated to Professor David Carrillo on the occasion of his 65th birthday.

## References and Notes

- (1) Sie, S. T. *Handbook of Heterogeneous Catalysis*; Ertl, G., Knözinger, H., Weitkamp, J., Eds.; Wiley-VCH: Weinheim, 1997; Vol. 4, p. 1998.
- (2) Arata, K.; Hino, M. *Proc. 9th Intern. Congress. Catal.*; Phillips, M. J., Ternan M., Eds.; The Chemical Institute of Canada: Ottawa, 1988; Vol. 4, p. 1727.
- (3) Hino, M.; Arata, K. *J. Chem. Soc., Chem. Commun.* **1988**, 1259.
- (4) Barton, D. G.; Soled, S. L.; Meitzner, G. D.; Fuentes, G. A.; Iglesia, E. *J. Catal.* **1999**, 181, 57.
- (5) Kuba, S.; Lukinskas, P.; Grasselli, R. K.; Gates, B. C.; Knözinger, H. *J. Catal.* **2003**, 216, 353.
- (6) Scheithauer, M.; Grasselli, R. K.; Knoezinger, H. *Langmuir* **1998**, 14, 3019.
- (7) Valigi, M.; Gazzoli, D.; Pettiti, I.; Mattei, G.; Colonna, S.; De Rossi, S.; Ferraris, G. *Appl. Catal. A* **2002**, 231, 159.
- (8) Baertsch, C. D.; Komala, K. T.; Chua, Y.-H.; Iglesia, E. *J. Catal.* **2002**, 205, 44.
- (9) Kuba, S.; Concepción Heydorn, P.; Grasselli, R. K.; Gates, B. C.; Che, M.; Knözinger, H. *Phys. Chem. Chem. Phys.* **2001**, 3, 146.
- (10) Okuhara, T.; Mizuno, N.; Misono, M. *Adv. Catal.* **1996**, 41, 113.

- (11) Baker, L. C. W. *Advances in the Chemistry of Coordination Compounds*; Kirschner, S., Ed.; Macmillan: New York, 1961.
- (12) Day, V. W.; Klemperer, W. G. *Science* **1985**, *228*, 533.
- (13) Klemperer, W. G.; Marquart, T. A.; Yaghi, O. M. *Angew. Chem.* **1992**, *104*, 51.
- (14) Baker, L. C. W.; Glick, D. C. *Chem. Rev.* **1998**, *98*, 3.
- (15) Pope, M. T. *Heteropoly and Isopoly Oxometalates*; Springer-Verlag: Berlin, 1983.
- (16) Errington, R. J. *Polyometalate Molecular Science*; Borrás-Almenar, J. J., Coronado, E., Müller, A., Pope, M. T., Eds.; Kluwer Academic Publishers: Dordrecht, 2003; p 55.
- (17) Hallopeau, L. A. C. R. *Acad. Sci.* **1896**, *1*, 1419.
- (18) Iball, J.; Low, J. N.; Weakley, T. J. R. *J. Chem. Soc., Dalton Trans.* **1974**, 2021.
- (19) Peacock, R. D.; Weakley, T. J. R. *J. Chem. Soc. A* **1971**, 1836.
- (20) Marcu, G.; Vatulesscu, R.; Budi, T. *Studia University Babes-Bolyai, Ser. Chem.* **1972**, *17*, 87.
- (21) Ripan, R.; Todorut, I. *Rev. Roum. Chim.* **1966**, *11*, 1279.
- (22) Chauveau, F.; Eberlé, J.; Lefebvre, J. *Nouv. J. Chim.* **1985**, *9*, 315.
- (23) Clegg, W.; Elsegood, M. R. J.; Errington, R. J.; Havelock, J. J. *Chem. Soc., Dalton Trans.* **1996**, 681.
- (24) Errington, R. J. *Rational Approaches to Polyoxometalate Synthesis*; Pope, M. T., Müller, A., Eds.; Kluwer Academic Publishers: Dordrecht, 2001; p 7.
- (25) Koningsberger, D. C.; Mojet, B. L.; van Dorsen, G. E.; Ramaker, D. E. *Top. Catal.* **2000**, *10*, 143.
- (26) Michalowicz, A. *Logiciels pour la Chimie*; Société Française de Chimie: Paris, 1991; p. 102.
- (27) Michalowicz, A. *J. Phys. IV France* **1997**, *7*, 235.
- (28) Sheldrick, G. M. *SHELXS-97*; Germany: University of Göttingen, 1997.
- (29) (a) Watkin, D. J.; Carruthers, J. R.; Betteridge, P. W. *CRYSTALS*; Chemical Crystallography Laboratory, University of Oxford: Oxford, 1996. (b) Pearce, L. J.; Watkin, D. J. *CAMERON*; Chemical Crystallography Laboratory, University of Oxford: Oxford, 1996.
- (30) Rocchiccioli-Deltcheff, C.; Thouvenot, R.; Dabbabi, M. *Spectrochim. Acta* **1977**, *33A*, 143.
- (31) Rocchiccioli-Deltcheff, C.; Fournier, M.; Franck, R.; Thouvenot, R. *J. Mol. Struct.* **1984**, *114*, 49.
- (32) Rocchiccioli-Deltcheff, C.; Fournier, M.; Franck, R.; Thouvenot, R. *Spectrosc. Lett.* **1986**, *19*, 765.
- (33) Mattes, V. R.; Bierbüsse, H.; Fuchs, J. Z. *Anorg. Allg. Chem.* **1971**, *385*, 230.
- (34) Li, M.; Feng, Z.; Xiong, G.; Ying, P.; Xin, Q.; Li, C. *J. Phys. Chem. B* **2001**, *105*, 8107.
- (35) Lefebvre, J.; Chauveau, F.; Doppelt, P.; Brévard, C. *J. Am. Chem. Soc.* **1981**, *103*, 4589.
- (36) Cadot, E.; Thouvenot, R.; Tézé, A.; Hervé, G. *Inorg. Chem.* **1992**, *31*, 4128.
- (37) Proust, A.; Thouvenot, R.; Roh, S.-G.; Yoo, J.-K.; Gouzerh, P. *Inorg. Chem.* **1995**, *34*, 4106.
- (38) Bustos, C.; Hasenknopf, B.; Thouvenot, R.; Vaissermann, J.; Proust, A.; Gouzerh, P. *Eur. J. Inorg. Chem.* **2003**, 2757.
- (39) Evans, J.; Pillinger, M.; Rummey, J. M. *J. Chem. Soc., Dalton Trans.* **1996**, 2951.
- (40) Fuchs, J.; Freiwald, W.; Hartl, H. *Acta Crystallogr., Sect. B* **1978**, *B34*, 1764.
- (41) Brown, I. D. *Structure and Bonding in Crystals*; O'Keeffe, M., Navrotsky, A., Eds.; Academic Press: New York, 1981; p. 1.
- (42) Brown, I. D.; Altermatt, D. *Acta Crystallogr., Sect. B* **1985**, *41*, 241.
- (43) McCullough, J. D.; Trueblood, K. N. *Acta Crystallogr.* **1959**, *12*, 507.
- (44) Morris, S.; Almond, M. J.; Cardin, C. J.; Drew, M. G. B.; Rice, D. A.; Zubavichus, Y. *Polyhedron* **1998**, *17*, 2301.
- (45) Kickelbick, G.; Wiede, P.; Schubert, U. *J. Chem. Soc., Dalton Trans.* **1999**, 1301 and references therein.
- (46) Shimomura, H.; Lei, X.; Shang, M.; Fehlner, T. P. *Organometallics* **1997**, *16*, 5302.
- (47) Martin, A.; Uhrhammer, R.; Gardner, T. G.; Jordan, R. F.; Rogers, R. D. *Organometallics* **1998**, *17*, 382.
- (48) Thorman, J. L.; Guzei, I. A.; Young Junior, V. G.; Woo, L. K. *Inorg. Chem.* **2000**, *39*, 2344.
- (49) Otero, A.; Fernandez-Baeza, J.; Antinolo, A.; Tejada, J.; Lara-Sanchez, A.; Sanchez-Barba, L.; Fernandez-Lopez, M.; Lopez-Solera, I. *Inorg. Chem.* **2004**, *43*, 1350.
- (50) Kholdeeva, O. A.; Maksimov, G. M.; Maksimovskaya, R. I.; Kovaleva, L. A.; Fedotov, M. A.; Grigoriev, V. A.; Hill, C. L. *Inorg. Chem.* **2000**, *39*, 3828.
- (51) Nomiya, K.; Takahashi, M.; Widegren, J. A.; Aizawa, T.; Sakai, Y.; Kasuga, N. C. *J. Chem. Soc., Dalton Trans.* **2002**, 3679.
- (52) Carrier, X.; Lambert, J.-F.; Che, M. *J. Am. Chem. Soc.* **1997**, *119*, 10137.
- (53) Carrier, X.; Lambert, J.-F.; Kuba, S.; Knözinger, H.; Che, M. *J. Mol. Struct.* **2003**, *656*, 231.
- (54) Scheithauer, M.; Cheung, T. K.; Jentoft, R. E.; Grasselli, R. K.; Gates, B. C.; Knözinger, H. *J. Catal.* **1998**, *180*, 1.
- (55) Barton, D. G.; Shtein, M.; Wilson, R. D.; Soled, S. L.; Iglesia, E. *J. Phys. Chem. B* **1999**, *103*, 630.
- (56) Barton, D. G.; Soled, S. L.; Iglesia, E. *Top. Catal.* **1998**, *6*, 87.
- (57) Afanasiev, P.; Geantet, C.; Breyse, M.; Coudurier, G.; Vedrine, J. C. *J. Chem. Soc., Faraday Trans.* **1994**, *90*, 193.